Engineering Structures 56 (2013) 2149–2153

Contents lists available at ScienceDirect

Engineering Structures

journal homepage: www.elsevier.com/locate/engstruct

Improvement of tuned mass damper by using rotational inertia through tuned viscous mass damper

Hernán Garrido, Oscar Curadelli, Daniel Ambrosini *

Struct. Eng. Master Program, Eng. Faculty, National University of Cuyo, Mendoza, Argentina
CONICET, National Research Council from Argentina, Argentina

ARTICLE INFO

Article history:
Received 20 October 2012
Revised 27 June 2013
Accepted 23 August 2013

Keywords:
Tuned mass damper
Tuned viscous mass damper
Frequency response
Effectiveness
SDOF
Rotational inertia

ABSTRACT

A new vibration control device called a rotational inertia double-tuned mass damper (RIDTMD) is proposed in this paper. The device consists of a tuned mass damper (TMD) in which the typical viscous damper is replaced with a tuned viscous mass damper. The linear model for a single-degree-of-freedom structure incorporating an RIDTMD, the equations of motion in state-space representations, and the transfer function of the considered model are derived. The optimum design parameters of the system subjected to harmonic load are obtained by using a numeric technique, and the performance of the new device is compared with that of a traditional TMD in terms of frequency response. The strokes of auxiliary masses are also assessed. Based on the results, it is demonstrated that the RIDTMD is more effective than a TMD at the same mass ratio, particularly at excitation frequencies near resonance. Moreover, the suppression band is wider and the moving block stroke is nearly identical for both devices.

1. Introduction

Mitigating the dynamic response of civil engineering and mechanical structures to earthquakes, wind, and rotating machinery has drawn the interest of many researchers in recent decades. Several passive, semi-active, and active control devices have been developed. Among the available devices, a TMD is one of the simplest and most reliable, typically consisting of an auxiliary mass, a spring, and a viscous damper attached to the structure to be controlled.

Hermann Frahm proposed the dynamic vibration absorber [1], later called the TMD, in the 1900s. Since then, several variant forms of TMDs have been proposed in order to improve performance. The Multiple Tuned Mass Damper (MTMD) was proposed and investigated by Xu and Igusa [2] and subsequently studied by several researchers [3–10]. In general, MTMDs are more effective and robust in mitigating the oscillations of structures than a single TMD.

Another type of TMD is the so-called double tuned mass damper (DTMD) or series tuned mass damper. This damper consists of one larger mass block (i.e., a larger TMD) and one smaller mass block (i.e., a smaller TMD) connected in a series. Li and Zhu [11] conducted research on the performance of a DTMD using a novel optimum criterion.

The working principle of all types of TMDs consists of transferring the vibration energy of the primary structure to an auxiliary mass-spring system (i.e., a TMD) in order to effectively dissipate the energy into a suitable damper. In the case of a traditional TMD, that damper is a linear viscous damper. However, other types of dampers can be used.

More recently, Hwang et al. [12] proposed to control structural vibrations by means of a rotational inertia viscous damper (RIVD) utilizing a ball screw amplifying mechanism. The authors noted that the efficiency of the RIVD heavily depended on the lead of the ball screw; as the lead decreases, the effectiveness of the damper significantly increases. Moreover, the apparent mass of the controlled structure, which also depends on the lead of the ball screw, is increased due to the installation of the RIVD.

Ikago et al. [13], based on the concepts of Hwang et al. [12], developed and studied the tuned viscous mass damper (TVMD), which is essentially an RIVD in series with a spring. The resulting apparent mass-spring arrangement behaves as a supplemental tuned oscillator that magnifies the deformation of the damper, thereby improving the performance of the RIVD. It is important to highlight that both devices, the RIVD and the TVMD, are two-terminal devices. For this reason they need a fixed reference to react, unlike the TMD which does not have that disadvantage.

* Corresponding author. Address: Facultad de Ingeniería, Centro Universitario, Parque Gral., San Martín, 5500 Mendoza, Argentina. Tel.: +54 2620 4559947; fax: +54 261 4380120.

E-mail address: dambrosini@uncu.edu.ar (D. Ambrosini).

0141-0296/$ - see front matter
http://dx.doi.org/10.1016/j.engstruct.2013.08.044

Other applications of rotational inertia can be found in the paper by Smith [14] in which, the two-terminal device which transforms rotational inertia in translational inertia is named "inerter".

In view of the features offered by the TVMD and the advantages of TMD, this paper proposes to replace the viscous damper in a traditional TMD with a TVMD, resulting in a rotational inertia double tuned mass damper (RIDTMD). The performance, in terms of the dynamic magnification factor (DMF) of the RIDTMD, is compared with a reference TMD on a single-degree-of-freedom (SDOF) system.

2. Mathematical models

2.1. TMD model

A schematic representation of a TMD coupled to an SDOF structure is shown in Fig. 1. The parameters k_s, c_s, and m_s are the stiffness, damping factor and mass of the structure to be controlled, respectively. Similarly, k_0, c_0 and m_0 are the stiffness, damping factor and mass of the TMD, respectively. The variables x_s and x_0 are the structure and TMD displacements, respectively; whereas f and $\ddot{x}_g$ denote the external force and support acceleration applied to the structure. In this paper, the model developed by Den Hartog [15] is used.

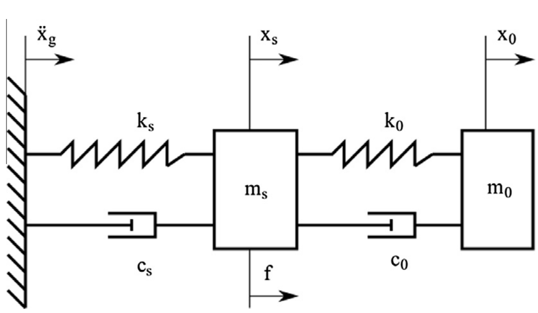

Fig. 1. TMD coupled to an SDOF structure.

2.2. RIDTMD model

Both the RIVD and the TVMD utilize a ball-screw mechanism that transforms an axial relative displacement into the rotational movement of a mass, which is in turn immersed in a viscous fluid that provides damping to the system [12]. The TVMD also includes a flywheel in order to increase its rotational moment of inertia and a secondary spring [13].

In this work, the damping of the RIVD is modeled by means of an axial dashpot [13] with an equivalent damping factor c_2, and the ball-screw mechanism is replaced with an equivalent pinion-rack mechanism in which the pinion radius r occupies the same role as the screw lead. The considered RIVD model, incorporating a flywheel, is shown in Fig. 2.

The following relation holds for the pinion-rack arrangement sketched in Fig. 2:

$$\theta = \frac{1}{r}(x_1 - x_2) \tag{1}$$

in which r and θ are the radius and the rotation angle of the pinion, and x_1 and x_2 are the displacements of each device end.

Fig. 3 shows an RIDTMD (i.e., a TMD using a TVMD) coupled to an SDOF system in which the moving block mass, the primary and secondary spring stiffness of the auxiliary system, and the equivalent damping factor of the RIVD are denoted by m_1, k_1, k_2, and c_2, respectively. The pinion, the immersed mass and the flywheel have their own translational masses, which are relatively small and can therefore be combined into m_1.

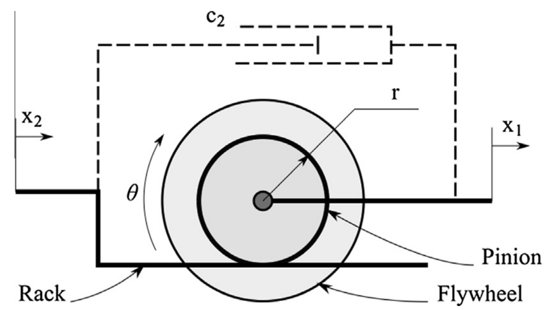

Fig. 2. RIVD incorporating a flywheel. The equivalent axial dashpot is in dashed line.

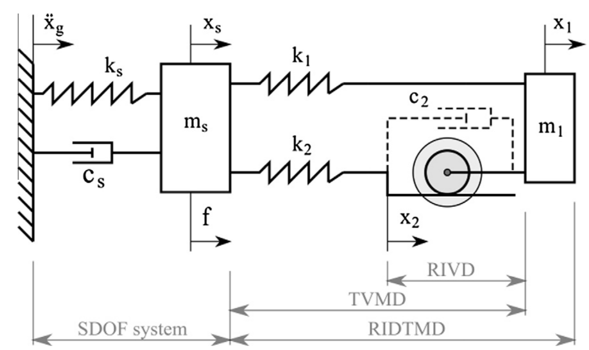

Fig. 3. An SDOF system incorporating an RIDTMD.

In the system sketched in Fig. 3, the potential and strain energies (U and T), the dissipative function ($\Im$), and the incremental work (δW) obtained when the external forces move through incremental displacements δx_i ($i = 1, 2, s$) are expressed as follows:

$$U = \frac{1}{2}k_s x_s^2 + \frac{1}{2}k_1(x_1 - x_s)^2 + \frac{1}{2}k_2(x_2 - x_s)^2 \tag{2}$$

$$T = \frac{1}{2}m_s\dot{x}_s^2 + \frac{1}{2}m_1\dot{x}_1^2 + \frac{1}{2}J\dot{\theta}^2 + \frac{1}{2}m_r\dot{x}_2^2 \tag{3}$$

$$\delta W = (f - m_s\ddot{x}_g)\delta x_s - m_1\ddot{x}_g\delta x_1 - m_r\ddot{x}_g\delta x_2 \tag{4}$$

$$\Im = \dot{x}_s c_s \delta \dot{x}_s + (\dot{x}_1 - \dot{x}_2)(\delta\dot{x}_1 - \delta\dot{x}_2)c_2 \tag{5}$$

in which J is the sum of the pinion, immersed mass, and flywheel rotational moments of inertia; m_r is the rack mass (which is neglected in this research); and x_i is the displacement in the degree-of-freedom i ($i = 1, 2, s$).

From expressions (1–5), and from defining the apparent mass as $m_2 = J/r^2$, the equations of motion are obtained as follows [16]:

$$k_s x_s + c_s\dot{x}_s + k_1(x_s - x_1) + k_2(x_s - x_2) + \ddot{x}_s m_s = -m_s\ddot{x}_g + f \tag{6}$$

$$k_1(x_1 - x_s) + c_2(\dot{x}_1 - \dot{x}_2) + m_2(\ddot{x}_1 - \ddot{x}_2) + \ddot{x}_1 m_1 = -m_1\ddot{x}_g \tag{7}$$

$$k_2(x_2 - x_s) + c_2(\dot{x}_2 - \dot{x}_1) + m_2(\ddot{x}_2 - \ddot{x}_1) = 0 \tag{8}$$

To find the transfer function of the system, the resulting system of differential equations is represented in state-space [17] as follows:

$$\dot{\mathbf{q}}(t) = \mathbf{A}\mathbf{q}(t) + \mathbf{B}u(t) \tag{9}$$

$$y(t) = \mathbf{C}\mathbf{q}(t) \tag{10}$$

where $\mathbf{q} = [\mathbf{x} \quad \dot{\mathbf{x}}]^T$ is the state vector, in which $\mathbf{x} = [x_s \quad x_1 \quad x_2]^T$; u is the system input load; y is the system output, i.e., the studied variable; $\mathbf{B}$ is the input matrix, which is determined by the applied load type; $\mathbf{C}$ is the output matrix, which depends on the selection of the studied variable; and $\mathbf{A}$ is the state matrix, which is given as follows:

$$\mathbf{A} = \begin{bmatrix} \mathbf{0}_3 & \mathbf{I}_3 \\ -\widehat{\mathbf{M}}^{-1}\widehat{\mathbf{K}} & -\widehat{\mathbf{M}}^{-1}\widehat{\mathbf{C}} \end{bmatrix} \tag{11}$$

where $\mathbf{0}_3$ and $\mathbf{I}_3$ are zero and identity 3×3 matrices, respectively, and $\widehat{\mathbf{M}}, \widehat{\mathbf{C}}$ and $\widehat{\mathbf{K}}$ are the mass, damping and stiffness matrices, respectively, as defined below.

For convenience, the following parameters are introduced:

$$\mu_1 = \frac{m_1}{m_s};\ \mu_2 = \frac{m_2}{m_s};\ \mu_{21} = \frac{m_2}{m_1} = \frac{\mu_2}{\mu_1};\ \alpha_1 = \frac{\omega_1}{\omega_s};\ \alpha_2 = \frac{\omega_2}{\omega_s};$$

$$\zeta_s = \frac{c_s}{2\omega_s m_s};\ \zeta_2 = \frac{c_2}{2\omega_2 m_2};$$

$$\omega_s = \sqrt{k_s/m_s};\ \omega_1 = \sqrt{k_1/m_1};\ \omega_2 = \sqrt{k_2/m_2}$$

The matrices $\widehat{\mathbf{M}}, \widehat{\mathbf{C}}$ and $\widehat{\mathbf{K}}$ can then be written as follows:

$$\widehat{\mathbf{M}} = m_s \begin{bmatrix} 1 & 0 & 0 \\ 0 & \mu_1 + \mu_2 & -\mu_2 \\ 0 & -\mu_2 & \mu_2 \end{bmatrix} \tag{12}$$

$$\widehat{\mathbf{C}} = m_s \begin{bmatrix} 2\zeta_s\omega_s & 0 & 0 \\ 0 & 2\mu_2\zeta_2\omega_2 & -2\mu_2\zeta_2\omega_2 \\ 0 & -2\mu_2\zeta_2\omega_2 & 2\mu_2\zeta_2\omega_2 \end{bmatrix} \tag{13}$$

$$\widehat{\mathbf{K}} = m_s \begin{bmatrix} \omega_s^2(1 + \mu_1\alpha_1^2 + \mu_2\alpha_2^2) & -\mu_1\omega_s^2\alpha_1^2 & -\mu_2\omega_s^2\alpha_2^2 \\ -\mu_1\omega_s^2\alpha_1^2 & \mu_1\omega_s^2\alpha_1^2 & 0 \\ -\mu_2\omega_s^2\alpha_2^2 & 0 & -\mu_2\omega_s^2\alpha_2^2 \end{bmatrix} \tag{14}$$

If an external dynamic force is applied to the structure (e.g., wind load or unbalanced rotating machinery), then $\mathbf{B}$ is given by expression (15) and $u = f$. If support acceleration is employed as an input (e.g., seismic load), then $\mathbf{B}$ is given by (16) and $u = \ddot{x}_g$.

$$\mathbf{B}_f = \begin{bmatrix} \mathbf{0}_{3\times1} \\ \widehat{\mathbf{M}}^{-1} \begin{bmatrix} 1 \\ 0 \\ 0 \end{bmatrix} \end{bmatrix} \tag{15}$$

$$\mathbf{B}_{\ddot{x}_g} = \begin{bmatrix} \mathbf{0}_{3\times1} \\ -\widehat{\mathbf{M}}^{-1} \begin{bmatrix} m_s \\ m_1 \\ 0 \end{bmatrix} \end{bmatrix} \tag{16}$$

Based on the above definitions, and taking into account that the system is linear and time-invariant, the generic transfer function (TF) and the frequency-response function in displacement are given, respectively, by the following expressions [17]:

$$H(s) = \frac{Y(s)}{U(s)} = \mathbf{C}(s\mathbf{I}_6 - \mathbf{A})^{-1}\mathbf{B} \tag{17}$$

$$H(j\omega) = H(s)|_{s=j\omega} \tag{18}$$

in which s is the Laplace variable, ω is the circular frequency, $j = \sqrt{-1}$, $\mathbf{I}_6$ is a 6×6 identity matrix, $Y(s)$ is the Laplace transform of the system output, and $U(s)$ is the Laplace transform of the system input.

In this research, the following TFs are used:

$$H_s(s) = [1 \quad 0 \quad 0 \quad 0 \quad 0 \quad 0](s\mathbf{I}_6 - \mathbf{A})^{-1}\mathbf{B}_f \tag{19}$$

$$H_{1s}(s) = [-1 \quad 1 \quad 0 \quad 0 \quad 0 \quad 0](s\mathbf{I}_6 - \mathbf{A})^{-1}\mathbf{B}_f \tag{20}$$

$$H_{2s}(s) = [-1 \quad 0 \quad 1 \quad 0 \quad 0 \quad 0](s\mathbf{I}_6 - \mathbf{A})^{-1}\mathbf{B}_f \tag{21}$$

To study the dynamic response of an RIDTMD, three main engineering parameters were selected. Specifically, two traditional responses of TMD-controlled structures are considered: structural displacement and auxiliary mass stroke. Moreover, because an RIDTMD is a two-degree-of-freedom device, two strokes must be studied.

If the output variable is the displacement of the structure (i.e., $y = x_s$), then the TF is given by (19). In a similar way, if the output variable is the stroke of the moving block (i.e., $y = x_1 - x_s$), then the TF is given by (20), and if the output variable is the stroke of the rack (i.e., $y = x_2 - x_s$), then the TF is given by (21).

Of course, many other TFs can be proposed for study. However, the study of structural displacement and auxiliary mass stroke is very common in existing literature. The structural displacement is the factor that designers strive to reduce in order to extend the structure's life. Additionally, the auxiliary mass stroke is also important because the required space for the installation of the control device is dependent on it.

For convenience, the dynamic magnification factor (*DMF*), which provides a dimensionless assessment of the dynamic response of the structure, is defined as follows:

$$DMF = k_s\|H_s(j\omega)\| \tag{22}$$

3. Optimization

To conduct a meaningful comparative assessment between the TMD and the RIDTMD, and because their performances are strongly dependent on the design parameters, an optimization procedure is required in each case

3.1. TMD optimization

The optimal parameters k_0 and c_0 that minimize the peak of the frequency-response function in displacement of the structure under harmonic force load are found by using Warburton's formulae [18] for mass ratios ($\mu = m_0/m_s$) of 1%, 5% and 10%. The optimal parameters are shown in Table 1 in a normalized form.

3.2. RIDTMD optimization

In this case, the same structural mass to auxiliary mass ratios μ_1 of 1%, 5% and 10% and the apparent mass to auxiliary mass ratios μ_{21} of 1%, 5%, 10%, 15%, 20%, 25% and 30% are considered. Note that the mass ratio of the RIDTMD (i.e., μ_1) has the same practical meaning as the mass ratio of the traditional TMD (i.e., μ) because both denote the relative mass added to the structure due the installation of the control device. Conversely, μ_{21} can be adjusted without altering the device weight; for instance, it can be modified by varying the fly-wheel radius.

Table 1
Optimum parameters of the TMDs.

$\mu = \frac{m_0}{m_s}$	$\alpha_0 = \frac{\omega_0}{\omega_s} = \sqrt{\frac{k_0 m_s}{k_s m_0}}$	$\zeta_0 = \frac{c_0}{2\sqrt{k_0 m_0}}$
0.01	0.9901	0.0609
0.05	0. 9524	0.1336
0.10	0.9091	0.1846

The design parameters to be optimized are k_1, k_2 and c_2. The optimization problem is then stated as follows:

$$\begin{array}{ll} \underset{[k_1 \quad k_2 \quad c_2]}{\text{minimize}} & \{J_0\} \\ & 0 < k_1 \leqslant k_{1_m}, 0 < k_2 \leqslant k_{2_m} \\ \text{subject to} & 0 \leqslant c_2 \leqslant c_{2_m}, \omega \in \Omega \end{array} \tag{23}$$

in which k_{1_m}, k_{2_m} and C_{2_m} are constants, and J_0 is the cost function defined as follows:

$$J_0 = \max_{\omega \in \Omega} \|H_s(j\omega)\| \tag{24}$$

where Ω denotes the range of possible exciting frequency ω.

The optimization problems are solved by using a sequential quadratic programming algorithm [19].

The optimized parameters are shown in Tables 2–4 in normalized form. Bold font cells refer to the cases in which the structure under an RIDTMD has the lowest response. Note that, in such cases, the primary subsystem (k_1, m_1) is tuned slightly below the natural frequency of the structure, whereas the secondary subsystem (k_2, m_2) is tuned slightly above the natural frequency of the structure. It can also be seen that α_1 and α_2 approach one when μ_1 approaches zero.

Table 4 shows that, for some smaller apparent mass to auxiliary mass ratios μ_{21}, the optimum damping ratio is greater than one (i.e., an over-critically damped case). Accordingly, the secondary subsystem does not oscillate and the RIDTMD behaves similar to a TMD. It is important to note that the minimum of J_0 occurs when the damping ratio is minimal.

4. Performance assessment

4.1. Effect of apparent mass to auxiliary mass ratio μ_{21}

To compare the effectiveness of the RIDTMD with respect to that of the TMD, the performance index R is defined as follows:

$$R = \frac{\max_{\omega \in \Omega} DMF_{(R)}(j\omega)}{\max_{\omega \in \Omega} DMF_{(T)}(j\omega)} \tag{25}$$

in which $DMF_{(R)}(j\omega)$ is the DMF of the structure which is controlled with an optimum RIDTMD (Section 3.2), and $DMF_{(T)}(j\omega)$ is the DMF of the structure which is controlled with an optimum TMD (Section 3.1).

The dependence of R on μ_{21} for systems provided with a TMD and an RIDTMD with the same mass ratios μ_1 and μ are displayed in Fig. 4. It is observed that the RIDTMD outperforms the TMD by approximately 20% in terms of performance index R. It is important to highlight that, in order to achieve the peak magnitude of the optimal RIDTMD with a 5% mass ratio μ_1, a traditional TMD would need a mass ratio μ of 7.9%, resulting in a 58% increase in m_0. Although the RIDTMD outperforms the TMD for all the studied values of μ_{21}, R displays the minimum values for μ_{21} between 10% and 15%.

Table 2
Optimum main tuning ratios (α_1).

μ_1	μ_{21}						
	1%	5%	10%	15%	20%	25%	30%
1%	0.933	0.946	**0.939***	0.911	0.893	0.866	0.852
5%	0.849	0.860	**0.925***	0.889	0.848	0.817	0.788
10%	0.757	0.715	0.873	**0.867***	0.822	0.785	0.742

* Cases in which the structure has the lowest response.

Table 3
Optimum secondary tuning ratios (α_2).

μ_1	μ_{21}						
	1%	5%	10%	15%	20%	25%	30%
1%	4.796	1.892	**1.008***	0.966	0.900	0.938	0.892
5%	6.914	2.966	**1.039***	1.089	1.042	0.992	0.949
10%	7.887	3.379	1.064	**1.077***	1.091	1.032	1.041

* Cases in which the structure has the lowest response.

Table 4
Optimum damping ratios (ζ_2).

μ_1	μ_{21}						
	1%	5%	10%	15%	20%	25%	30%
1%	2.398	0.881	**0.446***	0.621	0.593	0.853	0.863
5%	2.849	1.207	**0.241***	0.392	0.470	0.516	0.527
10%	3.411	1.959	0.200	**0.303***	0.415	0.456	0.560

* Cases in which the structure has the lowest response.

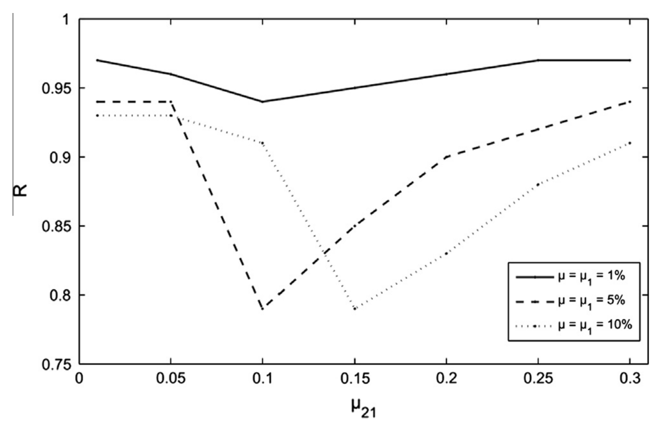

Fig. 4. R vs μ_{21} for TMDs and RIDTMDs with the same $\mu = \mu_1$.

It should be noted that, if a disk-shaped flywheel with radius $2r$ is used, then the mass of the flywheel is $0.5\mu_{21}m_1$. Consequently, the assumption that the mass of the flywheel can be part of, and therefore be lumped into, m_1 is true. Moreover, for the optimized value of μ_{21} = 10% the flywheel mass is much less than m_1 (only the 5% of m_1), as compared to the improvement in performance.

4.2. Structure response in frequency domain

It is important to show the performances of both optimum devices (RIDTMD and TMD) in terms of DMF (see Eq. (22)) for frequencies around resonance.

The Suppression Band (SB) is defined as the frequency range in which the structure controlled by the device (either TMD or RIDTMD) outperforms an uncontrolled structure. Fig. 5 shows the SBs of both devices. Note that there are undesirable zones where both a TMD-controlled and uncontrolled structure outperforms an RIDTMD. These undesirable zones can be defined approximately for frequency relations below 0.9 and over 1.1. However, this is not an actual disadvantage of RIDTMD because such undesirable zones can be avoided with a proper tuning of the device.

The DMF s of the systems provided with an RIDTMD and a TMD in the frequency ratio range of 0.5–1.5 and mass ratios $\mu = \mu_1$ of 5% are displayed in Fig. 5. It is noted that the structure provided with an RIDTMD has a considerably smaller DMF (approx. 20% smaller peaks) and wider SB (approx. 40% wider) than the structure provided with a TMD. The latter is because the frequency-response curve of the RIDTMD is flatter than that of the TMD.

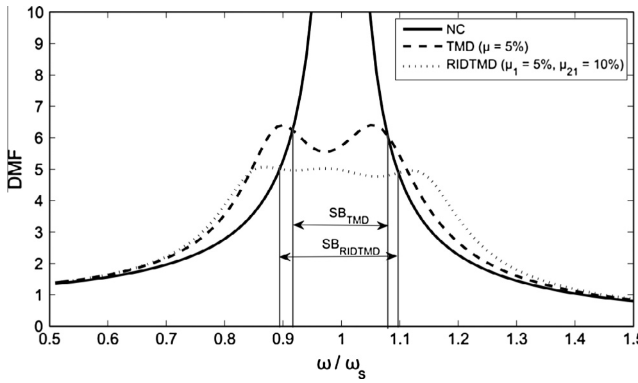

Fig. 5. Dynamic Magnification Factor of the controlled and non controlled structure.

Table 5
Assessment of the strokes.

μ_1, μ	J_b	J_r
0.01 (μ_{21} = 10%)	1.01	1.53
0.05 (μ_{21} = 10%)	0.97	2.27
0.10 (μ_{21} = 15%)	0.99	1.93

4.3. Device strokes

Because shorter strokes are desirable from a practical point of view, in this subsection the TMD and RIDTMD strokes are assessed by means of the following indicators (see Eqs. (20), (21)):

$$J_b = \frac{\max\limits_{\omega \in \Omega} \|H_{1s}(j\omega)\|}{\max\limits_{\omega \in \Omega} \|H_{0s}(j\omega)\|} \tag{26}$$

$$J_r = \frac{\max\limits_{\omega \in \Omega} \|H_{2s}(j\omega)\|}{\max\limits_{\omega \in \Omega} \|H_{0s}(j\omega)\|} \tag{27}$$

in which $H_{0s}(j\omega)$ is the frequency-response function in the displacements of the auxiliary mass of the TMD.

Considering the mass ratios μ and μ_1 of 1%, 5% and 10%, the results of the stroke assessments are presented in Table 5. It is observed that both the TMD and RIDTMD have nearly identical peak strokes. Conversely, the stroke of the rack is considerably larger than that of the auxiliary mass; however, this fact does not induce problems in practical applications because of the relatively small volume of the rack.

5. Conclusions

This paper proposed a device for vibration control (RIDTMD) in which the viscous linear damper of a traditional TMD is replaced with a TVMD. The advantages of the RIDTMD with respect to a traditional TMD are displayed in terms of DMF on SDOF systems under harmonic excitation.

The most important findings are listed below:

- The frequency-response curve of the RIDTMD is flatter than that of the TMD. Consequently, the peak of the DMF of the structure provided with an RIDTMD is approximately 20% lower and the SB is 40% wider than that of the structure provided with a TMD, with both having identical mass ratios and nearly identical auxiliary mass strokes.
- The apparent mass to auxiliary mass ratio μ_{21} of the RIDTMD plays a relevant role in the RIDTMD performance setting. The highest effectiveness is achieved for μ_{21} at approximately 10% for a typical mass ratio μ_1 (e.g., 1–5%).
- For the optimum μ_{21}, the mass of the rotational inertia is significantly small compared to the TMD mass. Then, with a quite simple addition to the traditional TMD, a significant improvement in performance is obtained.
- In general, the value of μ_{21} that minimizes the response of the structure also minimizes the optimum damping ratio ζ_2.

The device proposed in this paper (RIDTMD) could also be used in multi-degree-of-freedom (MDOF) structures. If the excitation and the structure are such that one mode of the structure is substantially more participating than the others, and the RIDTMD is properly tuned, one can expect to obtain similar results to the SDOF structural case. However, further study must be conducted in order to assess the performance of an RIDTMD in MDOF structures with many participating modes.

Acknowledgements

The financial support of CONICET and the National University of Cuyo is gratefully acknowledged. Special acknowledgements are extended to the reviewers of the first version of the paper because their useful suggestions led to improvements of the work.

References

[1] Frahm H. Device for damping vibrations of bodies, US Patent 989958; 1909.
[2] Xu K, Igusa T. Dynamic characteristics of multiple substructures with closely spaced frequencies. Earth Eng Struct Dyn 1992;21(12):1059–70.
[3] Li Chunxiang, Weilian Qu. Evaluation of elastically linked dashpot based active multiple tuned mass dampers for structures under ground acceleration. Eng Struct 2004;26(14):2149–60.
[4] Igusa T, Xu K. Vibration control using multiple tuned mass dampers. J Sound Vib 1994;175(4):491–503.
[5] Mohtat Arash, Dehghan-Niri Ehsan. Generalized framework for robust design of tuned mass damper systems. J Sound Vib 2011;330(5):902–22.
[6] Guo YQ, Chen WQ. Dynamic analysis of space structures with multiple tuned mass dampers. Eng Struct 2007;29(12):3390–403.
[7] Bakre SV, Jangid RS. Optimum multiple tuned mass dampers for base-excited damped main system. Int J Struct Stab Dyn 2004;4:527–42.
[8] Li Chunxiang, Weilian Qu. Optimum properties of multiple tuned mass dampers for reduction of translational and torsional response of structures subject to ground acceleration. Eng Struct 2006;28(4):472–94.
[9] Han B, Li C. Evaluation of multiple dual tuned mass dampers for structures under harmonic ground acceleration. Int J Struct Stab Dyn 2006;6(1):59–75.
[10] Park J, Reed D. Analysis of uniformly and linearly distributed mass dampers under harmonic and earthquake excitation. Eng Struct 2001;23:802–14.
[11] Li Chunxiang, Zhu Bilei. Estimating double tuned mass dampers for structures under ground acceleration using a novel optimum criterion. J Sound Vib 2006;298:280–97.
[12] Hwang JS, Kim J, Kim YM. Rotational inertia dampers with toggle bracing for vibration control of a building. Eng Struct 2007;29:1201–8.
[13] Ikago K, Saito K, Inoue N. Seismic control of single-degree-of-freedom structure using tuned viscous mass damper. Earth Eng Struct Dyn 2012;41(3):453–74.
[14] Smith MC. Synthesis of mechanical networks: the Inerter. IEEE Trans Autom Control 2002;47(10).
[15] Den Hartog JP. Mechanical vibrations. New York: Dover Press; 1985.
[16] Wright Jan R, Cooper Jonathan E. Introduction to Aircraft Aeroelasticity And Loads. Chichester, England: John Wiley & Sons Ltd.; 2007.
[17] Casciati F, Magonette G, Marazzi F. Technology of semiactive devices and applications in vibration mitigation. Chichester, UK: John Wiley & Sons, Ltd.; 2006.
[18] Warburton GB. Optimum absorber parameters for various combinations of response and excitation parameters. Earth Eng Struct Dyn 1982;10:381–401.
[19] Nocedal J, Wright SJ. Numerical optimization, 2nd ed. Springer Verlag: Springer Verlag; 2006. Springer Series in Operations Research.